

# Investigation of interference effects for a group of finite cylinders

A. Kareem<sup>a,\*</sup>, Tracy Kijewski<sup>a</sup>, Po-Chien Lu<sup>b</sup>

<sup>a</sup> *NatHaz Modeling Laboratory, Department of Civil Engineering and Geological Sciences, University of Notre Dame, 163 Fitzpatrick, Notre Dame, IN 46556-0767, USA*

<sup>b</sup> *Tamkang University, Taipei, Taiwan*

---

## Abstract

An experimental study of the interference effects between two and three cylinders of finite height immersed in a turbulent boundary layer at subcritical Reynolds numbers has been conducted in a boundary layer wind tunnel, utilizing a pneumatic averaging manifold system to measure the fluctuating force at various levels. Measurements of mean drag and lift force coefficients, mode-generalized RMS drag and lift force coefficients, and mode-generalized drag and lift force spectra, for a range of cylinder spacings, configurations, and various angles of attack, are presented. The interference levels observed were found to depend strongly on the spacing, angle of attack, and the arrangement of the cylinders with respect to each other. The investigation of these relationships for finite cylinders should prove insightful to those interested in such phenomena. © 1998 Elsevier Science Ltd. All rights reserved.

---

## 1. Introduction

Flow behavior around circular cylinders is a classical problem in fluid mechanics with a variety of practical applications, ranging from tall chimneys exposed to atmospheric boundary layer flows to cooling systems of nuclear reactors. In these situations the proximity of the adjacent structures under certain conditions introduces adverse or beneficial effects. From an aerodynamics perspective, a strong interaction takes place in the flow field around multiple body configurations that are sensitive to approach flow characteristics, as well as the angle of attack.

A host of studies have addressed the interference effects between two, three, and even four cylinders in uniform and/or turbulent flow [1–19]. Efforts in recent decades have been concerned with interference between finite cylinders, for which the

---

\* Corresponding author. E-mail: kareem@navier.ce.nd.edu.

additional feature of flow over the cylinder's top face is introduced [1]. At the top, the shear layer separates and interacts with the two layers which separate from the sides of the cylinder [2]. Still, while this phenomenon has been investigated, there is still a shortage of information on the aerodynamic characteristics of multiple finite cylinders.

In what experimental work that has been done, primary focus has been devoted to the influence of aspect ratio and cylinder spacing on aerodynamic behavior in subcritical, low-turbulence flows. The majority of this work has focused on the calculation of the mean and fluctuating pressure distributions on cylinders in tandem as described by Luo et al. [2]. Some attention has also been given to other configurations such as staggered and side-by-side alignments in work by Sun and Gu [3] and Sun et al. [4]. Still, the majority of work has been dedicated to the study of localized effects, with few studies giving primary consideration to lift and drag forces, especially their fluctuating components [5] and spectra. Furthermore, since most of the previous work was carried out in smooth flow, there is a shortage of information regarding the fluctuating forces on cylinders in turbulent boundary layer flows. This study then attempts to provide the needed information for multiple finite cylinders in a turbulent boundary layer.

This study considers this situation for groups of two and three cylinders of finite height and equal diameter, tested in a simulated boundary layer to investigate the aerodynamically induced fluctuating forces, as would be experienced by a group of chimney stacks. In particular, the present study details the relationship between cylinder spacing and arrangement (e.g. tandem, side-by-side, or staggered) and the level of interference which results, as reflected by the mean drag and lift coefficients, mode generalized RMS drag and lift coefficients, and the mode generalized drag and lift force spectra. All measurements are restricted to open country type flow, as the interference effects due to adjacent bodies are most pronounced in flows with low turbulence levels.

## 2. Experimental apparatus and method

The experiments were conducted in a boundary layer wind tunnel featuring a test section 4 ft 7 in high, 9 ft 10 in wide, and 47 ft long. The atmospheric boundary layer was simulated by passing the natural wind over surface roughness along the tunnel floor and past spires and barriers at the entrance to the testing section. The flow simulating an open country condition, possessed the flow characteristic presented in Table 1, where  $Re$  is the Reynolds number ( $D$  being the cylinder diameter,  $U_H$  the

Table 1  
Flow parameters

$Re = DU_H/\nu$	$\alpha$	$\sqrt{\bar{u}^2}/U$	$L_x/D$
$2.7 \times 10^4$	0.16	7%	4–7

velocity of the boundary layer at the cylinder height,  $H$  and  $\nu$  the kinematic viscosity),  $\alpha$  is the power law exponent,  $\sqrt{\bar{u}^2}/U$  describes the turbulence intensity, and  $L_x$  is the longitudinal integral length.

A 3 in  $\times$  30 in circular plexiglass cylindrical model, instrumented with pressure taps, was used for the wind load measurement. The dummy cylinders, serving as the adjacent interfering cylinders, were also constructed of plexiglass but without pressure taps. The measurement cylinder's height was divided into five levels, each with 14 pressure taps, placed such that groups of seven taps were located on each semi-circle of the cylinder, so that the tributary arc length for each tap resulted in an identical value of  $\sin(\phi)d\phi$ , in which  $\phi$  is the angle between the line joining the tap location and the origin with the horizontal axis, and  $d\phi$  is the arc angle subtended by the tributary arc length. Each of the seven pressure tap groups was connected to a seven-input manifold. The two manifolds facing one another on each level were connected to a pressure transducer to yield aerodynamic loads at that level. In this study, the levels along the height, at which local forces were measured by a manifolding technique, were spaced such that the summation of forces at that level provided appropriate weighting, resulting in a mode-generalized force. The pressure tubing and pneumatic averaging manifold were dynamically calibrated and their transfer function was directly incorporated in the signal processing to obtain high-frequency response for the system. The simultaneously measured output signals were passed through a low-pass filter, which were then digitized for subsequent analysis. The overall accuracy of this procedure can ideally be obtained by considering each component of the system, with the repeatability of each measurement considered as an assessment criterion for the accuracy. Thus, the repeatability of the local mean pressure coefficient was 0.1 and 0.03 for the RMS coefficient. A further discussion of other error estimates can be found in Ref. [1].

The mean drag and lift force coefficients were obtained separately through a summation of the five levels of pneumatically averaged area loads and then normalized with a factor of  $\frac{1}{2}\rho U_H^2 DH$ , where  $\rho$  is the density of air, and  $U_H$ ,  $D$  and  $H$  are as defined previously.

The spectra generalized with respect to a linear fundamental mode were obtained by covariance integration [1] which requires knowledge of the spanwise correlation and takes mode shape into account. The generalized RMS force was obtained by taking the square root of the generalized spectra, which was then normalized by a factor of  $\frac{1}{2}\rho U_H^2 DH$ , as defined above.

### 3. Test configurations

As outlined in Fig. 1, measurements were taken at  $\theta = 0^\circ, 10^\circ, 20^\circ, 30^\circ, 40^\circ$ , and  $90^\circ$  at spacings of  $S/D = 2, 3, 4, 5, 6$  and  $7$  for a set of two cylinders labeled configuration 1, where  $S$  is the distance between the centers of the cylinders and  $D$  is the diameter of the cylinders. For the case of three cylinders, a similar configuration (Fig. 1, configuration 2) was studied but for spacings only up to 5. In these scenarios, the observed cylinder

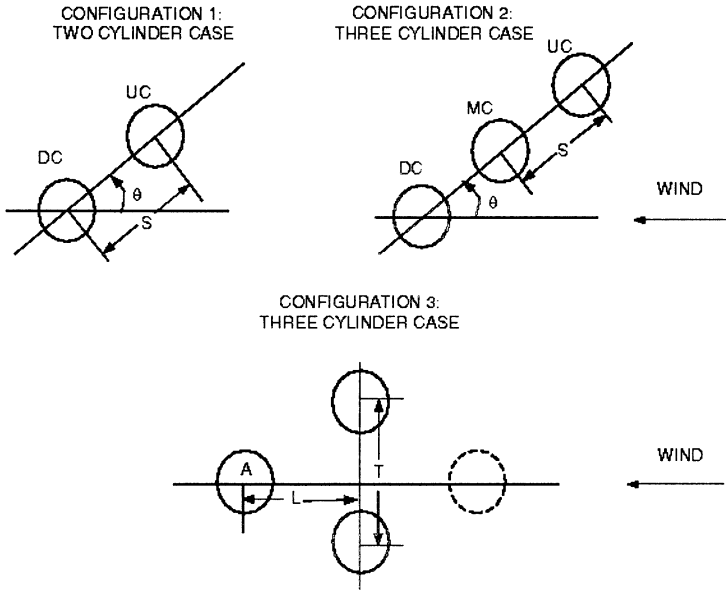


Fig. 1. Schematic of three cylinder configurations tested.

was one of three identical cylinders placed in line and located either at the middle or ends, with the spacing measured center to center symmetrically about the middle cylinder. A third configuration, three cylinders in a staggered arrangement, was also studied for two cases: cylinder A in either a windward or leeward position, also shown in Fig. 1. The cylinder under observation, cylinder A, was positioned in the centerline of the two side-by-side dummy cylinders, with longitudinal separations of  $L/D = -3, -2, 2, 3, 4$  and 5. The negative and positive signs correspond with the measurement cylinder being upstream and downstream of the two dummy cylinders, respectively. The two dummy cylinders were separated transversely at spacings of  $T/D = 2, 3$  and 4.

For all cases, the behavior of an isolated cylinder is presented for comparison. In the discussions which follow, although measurements were made for the incident angles of  $\theta$  mentioned above, a complete discussion of all the observations cannot be made for the sake of brevity. Likewise, while spectra and plots of the variation of the force coefficients with spacing were generated for all configurations studied, not all could be presented in this paper and are just commented on in passing.

## 4. Results and discussion

### 4.1. Configuration 1: Upstream cylinder of two cylinder configuration

The upstream cylinder (UC) in the two cylinder configuration, understandably, does not experience significant interference effects. The mean lift force for all spacings

and angles closely matches that of an isolated cylinder. In the tandem configuration, corresponding to a situation when  $\theta = 0^\circ$ , the RMS lift force significantly deviates from the values produced by other configurations, and only for a critical spacing of  $S/D = 2$ , converges to the values produced by all other angles for all other spacings. Even then, this range of values does not deviate significantly from that of an isolated cylinder. As for the mean drag force coefficient  $C_D$ , the values of all angles are tightly clustered and approach one another as the spacing increases, while always being less than or equal to that of an isolated cylinder. From this figure one may gauge that the upstream cylinder is only slightly subject to the influence of the downstream cylinder (DC) when the spacing between them is less than 4 cylinder diameters, in agreement with the findings of Taniguchi et al. [6]. For spacings less than this critical spacing,  $C_D$  is lower than that of isolated cylinder, as further illustrated by the RMS drag. Notice that for all angles, the generalized RMS drag force coefficient  $\tilde{C}_D$  converges to near that of an isolated cylinder at spacings greater than 4 diameters, indicating that the RMS drag of the UC is insignificantly affected by the presence of the downstream cylinder and only shows a slight reduction at small spacings. Note that in the tandem arrangement, once again at the critical spacing of 2 diameters, a maximum RMS drag force, greater than that of the isolated case, occurs.

The corresponding spectra also give some insight into the behavior of the upstream cylinder. From the alongwind spectra, one can observe that there is little discernible deviation from the spectra corresponding to an isolated cylinder (Fig. 2a). A peak at higher frequencies becomes more pronounced with increasing angle, while two high frequency peaks for  $S/D < 4$  appear when  $\theta = 30^\circ$  and become fully distinct at  $40^\circ$ .

In the acrosswind direction, the spectra show a shape similar to that of an isolated cylinder (Fig. 2b), but featuring a narrower peak that is greater in magnitude than the isolated case, for  $S/D > 3$ , as vortices begin to shed periodically from the upstream cylinder. Interference will then commence in the fully turbulent wake region. Suppressed vortex shedding at  $S/D \leq 3$  is characterized by the broader peak in the generalized spectra in the acrosswind direction for the UC, but this peak does tend to narrow as the angle increases.

#### 4.2. Configuration 1: Downstream cylinder in two cylinder configuration

More interesting interference effects are manifested for the downstream cylinder as it is buffeted by the wake from the upstream cylinder. A critical situation is encountered in the tandem arrangement, in which case the cylinders are one behind the other in the oncoming flow, creating a situation where the downstream bodies are enveloped in the wake of the upstream cylinder. In such instances, one would expect the interference of the flow between the cylinders to be closely connected to the properties and behavior (e.g. shear layers, vortex formation, etc.) of the upstream wake [7], with the mean drag forces decreasing remarkably at small spacings and for small angles [6,8]. From Fig. 3 one can see that, at small spacings near the tandem configuration, the mean drag is nearly zero and does experience marked variation in comparison to the upstream cylinder, with the minimum mean drag force occurring in this tandem

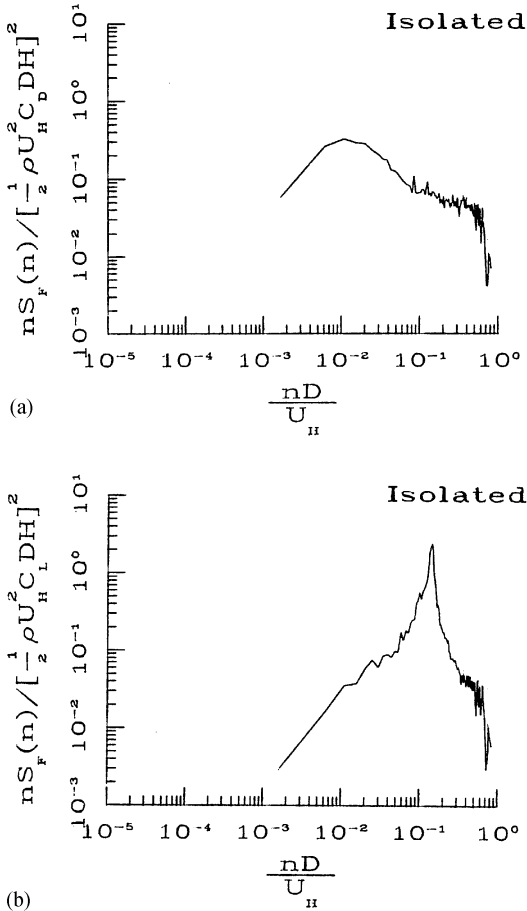


Fig. 2. (a) Spectra of RMS drag coefficient on isolated cylinder. (b) Spectra of RMS lift coefficient on isolated cylinder.

configuration for all spacings. This minimum drag value is also closely followed by the values of the near-tandem 10° configuration. The phenomena is in part caused by the shielding effect due to the proximity of the two cylinders. Furthermore, for greater spacings, the turbulence spawned by the UC promotes attachment of flow onto the downstream cylinder creating a change in pressure distribution which translates into a rapid decrease in the drag force. Although this study did observe a minimum mean drag force in the tandem configuration, the minimum drag coefficient observed by Zdravkovich [9] occurred in the staggered arrangement for two 2D cylinders in a uniform flow. Similarly, a study by Sun and Gu [10] observed a minimum drag force between 5° and 10°, which, although staggered, is close to the tandem configuration, in agreement with the findings presented here.

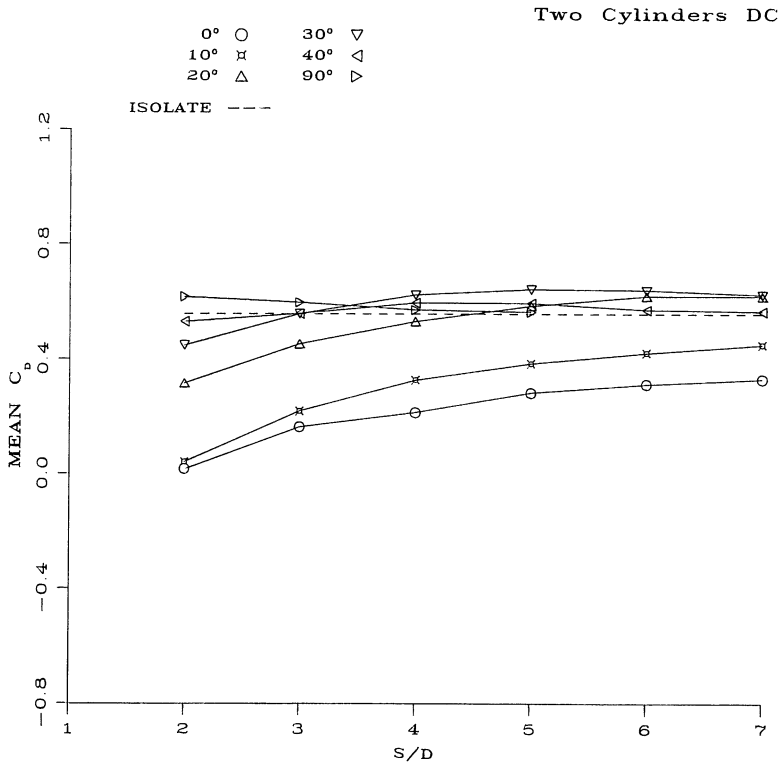


Fig. 3. Mean drag force coefficient on downstream cylinder – configuration 1.

As the angle of attack increases, so does the mean drag, exceeding the values measured for isolated cylinders, reaching a maximum value for spacings greater than 4 diameters at an angle of 30°. Similarly, the buffeting effect of the upstream wake on the DC in general shows a fluctuating drag force greater than that of an isolated cylinder, irrespective of the spacing, as illustrated by Fig. 4. For all configurations except side-by-side ( $\theta = 90^\circ$ ), the RMS drag reaches a maximum at  $S/D = 4$  and then slowly decays, in agreement with other studies [5,9]. The RMS drag force is maximum for spacings of 3 and 6 diameters at an angle of 20°, with small spacings of 2 diameters experiencing a maximum RMS drag in the tandem configuration. In a situation when the cylinders are side-by-side ( $\theta = 90^\circ$ ), the DC cylinder essentially behaves like an isolated one.

As demonstrated by Fig. 5, in the side-by-side arrangement for small spacings, the mean lift force coefficient  $C_L$  marginally exceeds that of an isolated cylinder, while an angle of 30° coupled with a sufficiently large spacing (5 diameters), is the only other configuration whose mean lift exceeds that of an isolated case. It can also be observed that the mean lift force becomes more negative as the downstream cylinder approaches the upstream wake at small separations. A maximum negative lift on the DC

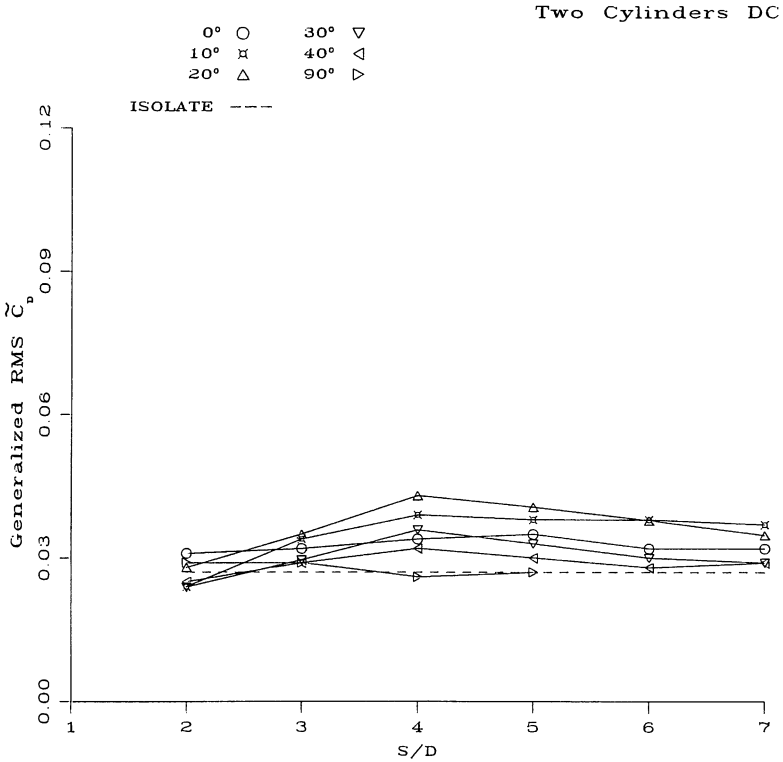


Fig. 4. RMS drag force coefficient on downstream cylinder – configuration 1.

occurs for the near-tandem 10° configuration, closely paralleled by the 20° configuration, whose values converge to that of an isolated cylinder at large spacings ( $S/D = 7$ ). This trend shows agreement with that of Bokian and Geoola [8], Taniguchi et al. [6], and Zdravkovich and Pridden [9]. Ishigai et al. [11] also observed this trend for a tandem arrangement with critical spacing being 3.8 diameters, noting the development of vortex streets behind both cylinders at equal values of the vortex shedding frequency. This flow behavior may be classified into two regimes: for spacings up to the critical spacing, the vortex street is suppressed behind the front cylinder and beyond this critical spacing, both cylinders form vortex streets [7]. In the side-by-side arrangement, other studies have also observed that for sufficiently wide spacings (typically beyond 3.5  $S/D$ ), the two cylinders form their own vortex streets independently, like that of an isolated cylinder [7]; however, at diminished spacings, antiphase vortex shedding appears (the production of vortices of opposite sign by each cylinder, simultaneously). As spacing increases, the DC cylinder in a side-by-side arrangement manifest mean lift force coefficients that approach that of an isolated cylinder. While this symmetry is maintained for spacings of 2 diameters, even closer spacings result in a flow biased to one side with a large scale Karman vortex street formed some

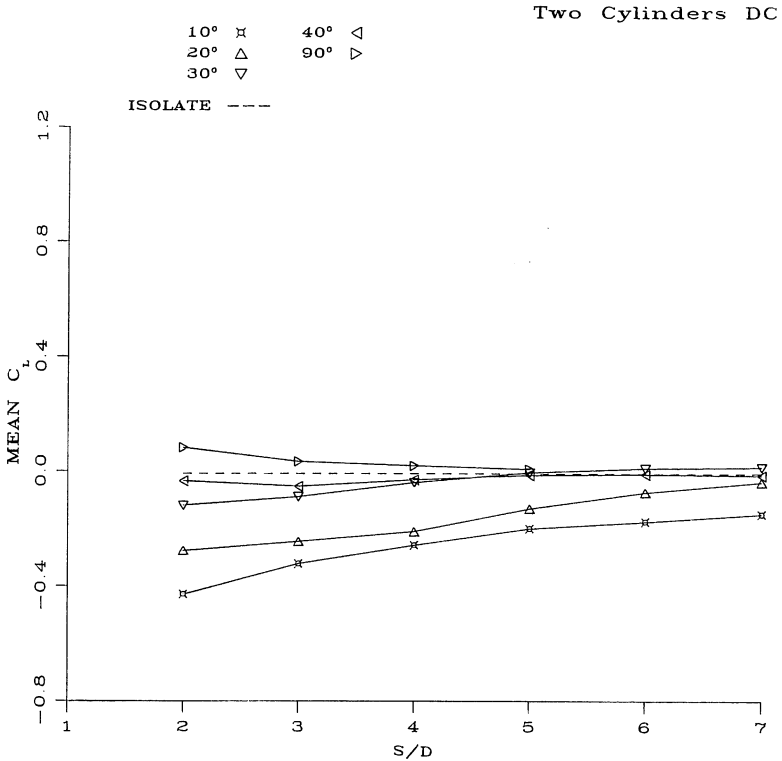


Fig. 5. Mean lift force coefficient on downstream cylinder – configuration 1.

distance downstream. At very small spacings, the gap flow is weak and separated shear layers on the outside of both cylinders interact with each other and roll up to form a large-scale vortex, thus yielding the behavior of an isolated cylinder. Such bistable behavior are also reflected in the drag and lift coefficients. The cylinder on the biased side experiences larger drag and lift forces that are associated with a narrower wake, the converse being true for the cylinder on the unbiased side [7]. This biased flow phenomena was also observed in side-by-side arrangements at supercritical Reynolds numbers in a study by Sun and Gu [10].

On the other hand, the RMS lift force coefficient, represented by Fig. 6, shows great variation. The generalized RMS lift force coefficient ( $\bar{C}_L$ ) for the DC is reduced for all angles at spacing ratios less than 3. The reduction of these fluctuating forces are a result of the vortex shedding from the upstream cylinder being suppressed at small separations due to the obstruction introduced by the downstream cylinder. In this range of spacing, the maximum RMS lift is in the near-tandem configuration, while beyond this critical spacing, the maximum RMS lift occurs at 20°. As the spacing increases from 2 diameters to 4, there is a rapid increase in RMS lift. Beyond  $S/D = 4$ , the RMS lift values for angles of 30° and 40° fall off rapidly while those of the near tandem arrangements of 10° and 20° hold fairly constant.

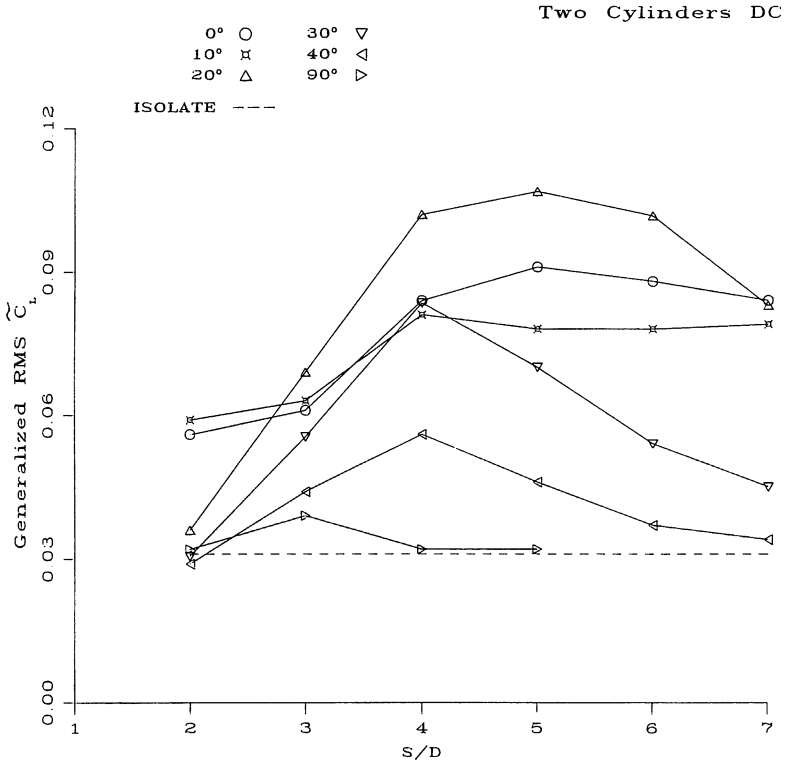


Fig. 6. RMS lift force coefficient on downstream cylinder – configuration 1.

Another exceptional feature surfaces for the DC in the tandem arrangement: both the RMS drag and lift forces at  $S/D = 2$  are larger in comparison to the isolated cylinder, while, for  $S/D = 3$ , they converge to a narrower range of values produced by other angles. A similar observation was also made by Arie et al. [5]. It is not surprising that both the drag and lift force fluctuations indicate high interference. When  $\theta = 20^\circ$ , the downstream cylinder experiences the highest RMS drag and lift between  $S/D = 3$  to 6. It is noted that both the RMS drag and RMS lift peak for flow approaching at  $\theta = 20^\circ$ . In this configuration, the shear layer of the UC has maximum impact on the DC forces.

Examination of the spectra for the downstream cylinder affirms the trends detected from the force coefficients. While the DC spectra show similar trends to the UC, the acrosswind spectrum of the downstream cylinder exhibits a peak which is slightly higher and exceptionally narrow compared to the isolated cylinder (Fig. 2b) indicating a particularly strong periodicity and coherence of the vortex shedding along the cylinder height. At  $S/D \leq 3$ , the sharp peak is suppressed and diminishes in magnitude with a broader band, as shown by Fig. 7. At  $S/D < 3$  with  $\theta = 10^\circ$  and  $20^\circ$ , the peak does not appear. As the cylinders approach a side-by-side configuration ( $\theta = 90^\circ$ ), the

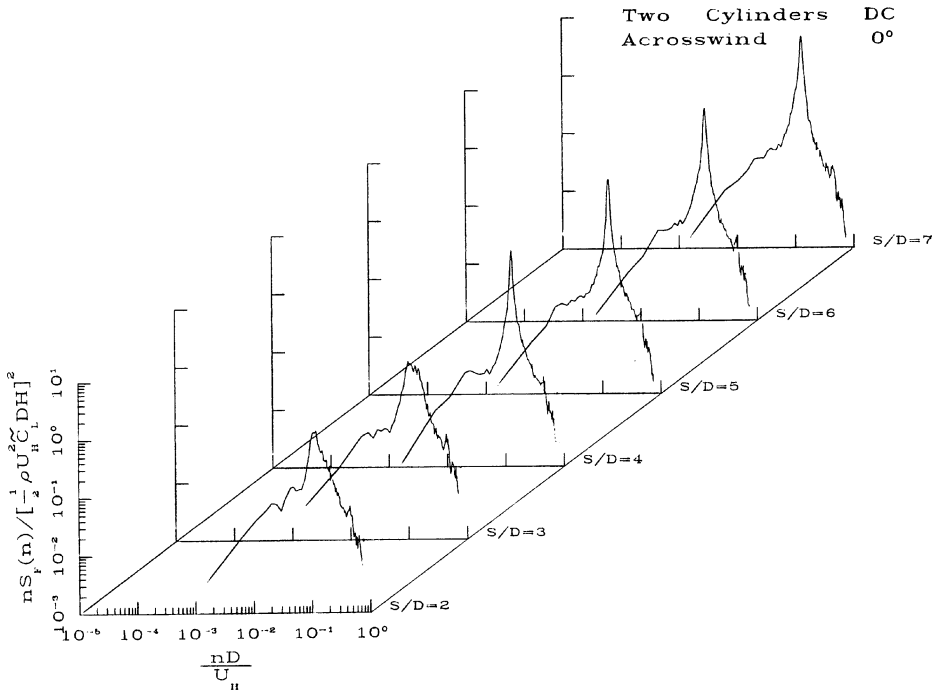


Fig. 7. Spectra of RMS lift coefficient on downstream cylinder for an angle of  $0^\circ$  – configuration 1.

interference between the cylinders becomes negligible for  $S/D \geq 2$ , in support of previous observations. This is manifested by the spectra closely resembling that of an isolated cylinder.

Conversely, the alongwind spectrum of the downstream cylinder near the tandem arrangement has a pronounced peak in the vicinity of double the shedding frequency or so called longitudinal mode. Upon approach flow angle change, the downstream cylinder facilitates a gap flow which is biased towards itself. The axes of the vortex shedding of the downstream cylinder skewed away from the centerline of the wake; therefore, the alongwind spectra of the downstream cylinder shows a fundamental peak at a frequency corresponding to the vortex shedding coupled with a second harmonic peak at twice of the shedding frequency. This second peak is highly discernible for  $S/D > 3$  when  $\theta = 10^\circ$  (Fig. 8) and  $20^\circ$ . The first peak diminishes in magnitude with increasing  $S/D$  and  $\theta$ , becoming almost indiscernible for  $S/D > 5$  and  $\theta = 30^\circ$  and  $S/D > 4$  with  $\theta = 40^\circ$ . Depending on the angle of attack, the wake of the UC begins to interact with the flow over the DC, thus modifying its wake. With increasing angle of the approach flow, additional harmonics in the spectra begin to appear. The corresponding spectra reveal that the amplitude of peaks at the frequency corresponding to vortex shedding and a second harmonic peak at twice the shedding frequency are sensitive to the spacings resulting in a redistribution of spectral energy in the side-by-side configuration.

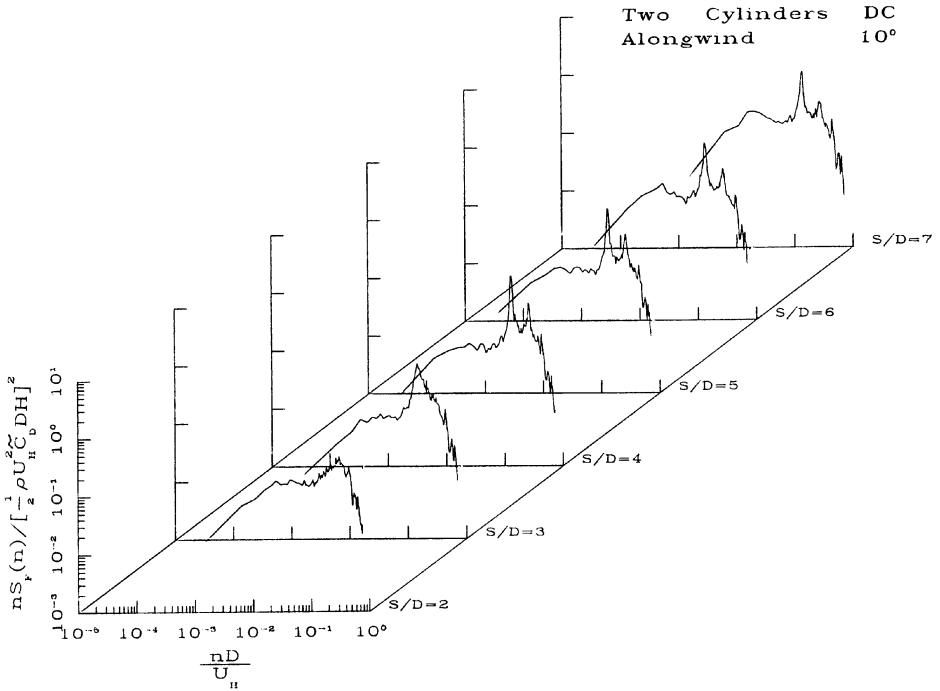


Fig. 8. Spectra of RMS drag coefficient on downstream cylinder for an angle of 10° – configuration 1.

### 4.3. Configuration 2: Middle cylinder in three cylinder configuration

Referring to Fig. 1, the configuration described herein features three cylinders in a line. The interference effects on the middle cylinder (MC) and downstream or third cylinder are of primary interest and will be discussed here, beginning with the middle cylinder. It may be noted that the interference acting on the middle cylinder is much the same as that of the downstream cylinder in the two cylinder case, with the mean drag reflecting its lowest values for the tandem and near tandem 10° configurations and gradually increasing with increased spacing. On the other hand, all other angles approach the mean drag force coefficient values produced by the isolated cylinder as the spacing increases. For the most part,  $\theta = 40^\circ$  produces a situation most like the isolated case, with little deviation as the spacing increases. Referring to the RMS drag force coefficients, one may observe that the values are closely clustered and their distribution tightens as the spacing diminishes. The peak RMS drag is experienced at 20° for a spacing of 4 diameters.

An examination of the mean lift force indicates that the mean lift is negative for nearly all spacings and angles, becoming most negative for all spacings at 10°. When in a side-by-side configuration, the MC behaves as an isolated cylinder, with respect to mean lift forces. As the spacing increases, observe how the mean lift forces approach

the values produced by the isolated cylinder, with values for  $\theta = 40^\circ$  converging with that of  $\theta = 30^\circ$  beyond 3 diameters. On the other hand, the RMS lift force undergoes a wide range of values with behavior that almost exactly parallels that of the DC in the two cylinder case. Once again, there is a rapid increase in the RMS lift for angles of  $20^\circ$  and  $30^\circ$  up to  $S/D = 4$  after which the value of  $\theta = 30^\circ$  falls off. A similar trend, though not as drastic, is experienced by angles of  $40^\circ$  and  $90^\circ$ . The tandem and near tandem configurations also gradually increase approaching  $S/D = 4$ . A peak RMS lift is encountered at  $S/D = 5$  for an angle of  $20^\circ$ , with values of the RMS lift being greater than the isolated case for nearly all spacings.

Before moving on to the DC, the spectra of the acrosswind and alongwind forces for the middle cylinder will also be discussed. The alongwind spectra manifests a peak that is broader and reduced, in comparison with the isolated cylinder (Fig. 2a), for small angles. As the angle increases to  $20^\circ$ , two sharp narrow peaks begin to appear at spacings greater than 3 diameters, but later disappear as the angle increases further. On the other hand, the acrosswind spectra manifests an exceptionally narrower and higher peak than the isolated cylinder (Fig. 2b), with the appearance of additional harmonics at higher frequencies as the angle increases.

#### 4.4. Configuration 2: Downstream cylinder in three cylinder configuration

The mean drag force coefficient on the downstream cylinder is less than that of an isolated cylinder at small spacings ( $S/D = 2$ ), but at larger spacings ( $S/D \geq 4$ ), angles of  $20$ – $40^\circ$  exceed those values. The maximum negative mean drag on both the MC and DC occurs for  $S/D \geq 3$  at  $\theta = 0^\circ$ . When the three cylinders are in this tandem or near tandem configuration, there is little variation in the mean drag, regardless of spacing. While this holds true for the tandem configuration, with respect to the RMS drag force, the near tandem  $10^\circ$  configuration experiences a gradual increase in RMS drag for spacings up to 4 diameters. Similar trends are experienced by the  $20^\circ$ ,  $30^\circ$ , and  $40^\circ$  configurations. It is readily observed that the tandem arrangement behaves very much like an isolated cylinder with respect to RMS drag.

The mean lift of the end or downstream cylinder in the three cylinder case exhibits only a slight difference from values for the MC, discussed previously, with a negative drag force experienced for nearly all spacings and angles, reaching a maximum negative value at  $10^\circ$  for all spacings. Note that at  $40^\circ$ , the mean drag force on the downstream cylinder is nearly that of an isolated case, with little variation as the spacing changes. All other angles gradually approach the values of the isolated cylinder as spacing increases toward 5 diameters. On the other hand, there are marked variations in the RMS lift force on the downstream cylinder. The RMS lift coefficient of the DC is greater than that of the MC, especially for  $\theta = 30^\circ$ , in which case the value of the RMS lift coefficient on the DC increases rapidly and becomes comparable with the RMS lift for the DC at  $\theta = 20^\circ$  at  $S/D = 4$ , where the RMS lift forces peak. These two angles experience a rapid increase approaching the critical spacing of 4 diameters, beyond which, values of  $\theta = 30^\circ$  fall off sharply to a level as low as those for  $0^\circ$  and  $10^\circ$ . A similar trend may also be observed, though with markedly lower values, for the  $40^\circ$  configuration. The tandem and near tandem  $10^\circ$  configurations follow each other

closely, experiencing a gradual escalation in RMS lift with increased spacing. The RMS lift coefficients for  $0^\circ$  and  $10^\circ$  have a considerably high value for the MC, but they decrease for the DC. Still, the maximum RMS lift and drag on the DC and MC occur for  $\theta = 20^\circ$  and  $S/D > 3$ .

This discussion is further enriched by examining the corresponding spectra for the downstream cylinder in this three cylinder configuration. The presence of the two cylinders in front of the third one understandably gives rise to a complex flow field. The acrosswind spectra of the DC shows an increase in magnitude at low frequencies when compared to the isolated case, but the shedding level remains the same. The low-frequency peaks are primarily resulting from the increase in the lateral turbulence level. As the angle and spacing increase, the peak in the spectra increases in magnitude and becomes markedly narrower. The alongwind spectra of the DC shows similar trends as the MC with an even broader and reduced peak for small angles. In addition, two peaks become discernible as the angle and spacing increase.

#### 4.5. Configuration 3: Three cylinders

The final configuration that will be considered is a three cylinder configuration (configuration 3) shown in Fig. 1 that features two dummy cylinders, side-by-side, positioned either upstream or downstream of the measurement cylinder. The mean lift force for this particular configuration is zero due to symmetry; however, measurements of the RMS lift may still be gaged. When the measurement cylinder is located upstream of the two dummy cylinders, a situation indicated by negative values of  $L/D$ , the deviation of the RMS lift from that of the isolated case is not incredibly significant, even for the three different transverse spacings considered. On the other hand, the RMS lift increases markedly once the measurement cylinder is behind the two dummy cylinders in the oncoming flow. At transverse spacings of two diameters, the RMS lift peaks at  $L/D = 3$  and then falls off while  $T/D = 3, 4$  both peak at  $L/D = 4$ .

As for the mean drag force, once again significant deviation from the isolated case occurs only when the two dummy cylinders are upstream of the test cylinder. For  $T/D = 2$  notice how the drag diminishes toward zero as  $L/D$  increases, while  $T/D = 4$  surfaces as a critical spacing for which the test cylinder behaves as an isolated one. The total drag is greater as the spacing ratio increases because each cylinder tends to behave as an isolated one [12]. The RMS drag affirms that transverse spacing has little effect when the dummy cylinders are downstream from the test cylinder, with the values being closely clustered and near that of the isolated case for all negative  $L/D$  spacings. Once the dummy cylinders are placed in front of the test cylinder, there is a significant increase in RMS drag for transverse spacings of 3 diameters. While  $T/D = 4$  does also experience a steady increase in RMS drag, though not as drastic, the transverse spacing of 2 peaks at a longitudinal spacing of 3 and then falls off, approaching the values produced by the isolated cylinder as the distance between the dummy cylinders and the test cylinder increases.

In the subsequent discussions of the alongwind and acrosswind spectra, the cases of interest are only those in which the two dummy cylinders are placed upstream of the

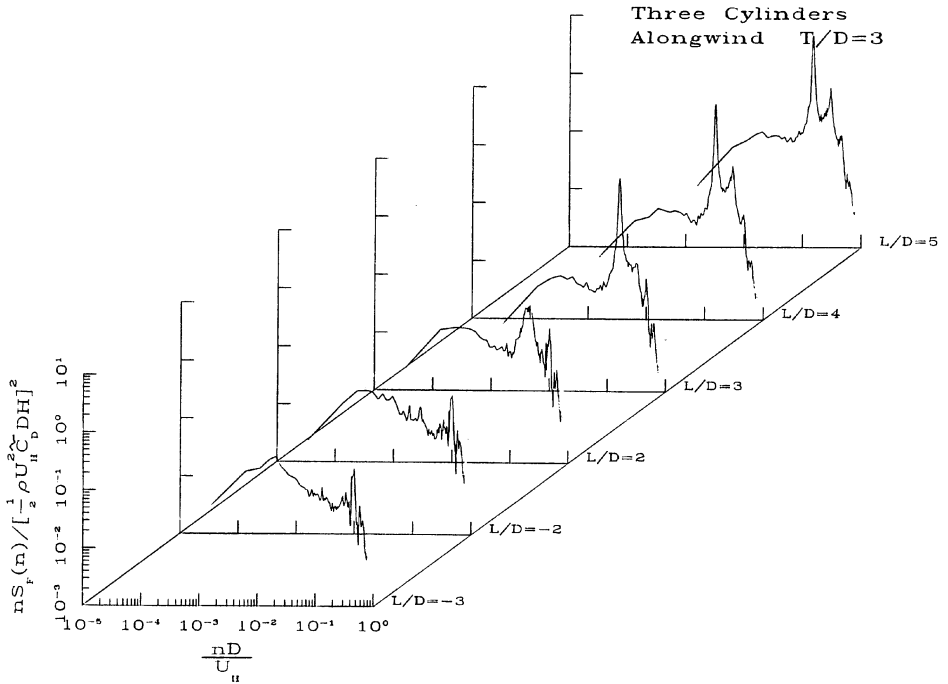


Fig. 9. Spectra of RMS drag coefficient on test cylinder for  $T/D = 3$  – configuration 3.

test cylinder, since the other scenario yields uninteresting results closely matching the behavior of the isolated cylinder (Fig. 2a and 2b). It is interesting to note that the alongwind spectra shows a very high peak at the shedding frequency and a second peak, albeit decreased in magnitude, at the double shedding frequency, clearly seen for  $L/D > 3$  (Fig. 9). The energy level of the harmonic peak at  $T/D > 2$  and  $L/D > 2$  is even higher than that of the acrosswind spectra. This feature indicates that very well organized vortices from the two upstream cylinders buffet the downstream cylinder, resulting in a narrow peak in the spectrum at their frequency.

When the spacing is decreased, the acrosswind spectra for the measurement cylinder at the upstream position show a suppressed peak, while the spectra for the cylinder at the downstream  $L/D = 2$  and 3 and  $T/D = 2$  and 3 indicate that the peak at the shedding frequency disappears, with two peaks, one at half the shedding frequency and the other at twice the shedding frequency, appearing (Fig. 10). Both involve a somewhat complex flow pattern that nevertheless exhibits a quasi-order nature. Further downstream, the spectra contain a peak at the shedding frequency with amplification of the energy level both at lower and higher frequencies in comparison to the isolated cylinder. As the transverse spacing increases to 4 diameters, however, these peaks begin to diminish and with increased longitudinal spacing, the test cylinder behaves as an isolated one.

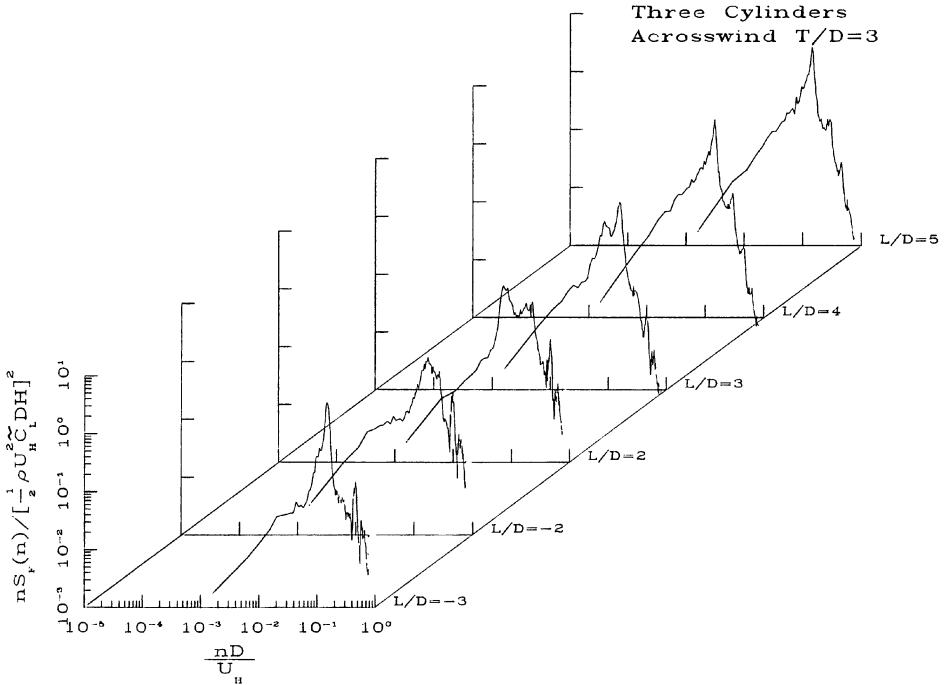


Fig. 10. Spectra of RMS lift coefficient on test cylinder for  $T/D = 3$  – configuration 3.

## 5. Conclusions

### 5.1. Two cylinder case

This study examines the level of interference due to proximity effects in a boundary layer flow for aerodynamic quantities such as mean and RMS lift and drag and their spectral descriptions. The most interesting phenomena involved the downstream cylinder, whose mean lift and drag coefficients are in general agreement with previous studies, with a minimum drag being experienced in tandem and near-tandem configurations. The maximum mean drag was found for  $S/D = 4$ . Large values of generalized RMS lift and drag coefficient occur when the measurement cylinder is buffeted by the wake of the upstream cylinder, with maximum values of the occurring at an angle of  $20^\circ$  and spacings between 3 and 4 diameters.

The spectra reveal that there is vortex formation, and these vortices do impinge on the measurement cylinder. For smaller separations, such as  $S/D < 3$ , the vortex shedding of both the upstream and downstream cylinders has been suppressed; however, when the downstream cylinder is positioned at a spacing ratio greater than three, the vortex shedding of the downstream cylinder is enhanced, whereas the upstream cylinder is hardly affected. Due to the vortex impingement, the downstream

cylinder is subjected to alongwind fluctuations at the shedding frequency and twice the shedding frequency.

### 5.2. Three cylinder cases

Effects similar to those found in the two cylinder case were found for the second cylinder in an in-line arrangement of three cylinders (configuration 2). There is only small difference between the middle cylinder and the downstream cylinder in configuration 2, except for the DC being affected more by low-frequency fluctuations. Peak RMS drag and lift forces were witnessed at  $20^\circ$  and  $S/D > 3$ , but the RMS lift on the DC was greater than that on the MC. The middle cylinder did experience RMS lift forces just like the DC in configuration 1, the two cylinder case.

When the downstream cylinder is exposed to the dual wakes of the two side-by-side upstream cylinders, as configuration 3 simulates, it manifests signs of significant interference. While symmetry eliminates the mean lift force, a peak RMS lift is once again experienced at the critical spacing of  $L/D = 3 - 4$ . The mean drag force can be practically diminished to zero when the transverse spacing of the dummy cylinders is 2 diameters while the RMS drag at a transverse spacing of 3 diameters shows a drastic increase as the longitudinal spacing increases. The spectra reflect a large alongwind fluctuation which is comparable with the acrosswind fluctuation at the shedding frequency. For small separations,  $S/D < 3$ , the spectra of the downstream cylinder exhibit double peaks at half the shedding frequency and twice the shedding frequency.

### Acknowledgements

The support for this work was provided in part by NSF Grant CMS94-02196 and CMS95-03779 and their REU supplements.

### References

- [1] A. Kareem, C.M. Cheng, Po Chien Lu, Pressure and force fluctuations on isolated circular cylinders of finite height in boundary layer flows, *J. Fluids Struct.* 3 (1989) 481–508.
- [2] S.C. Luo et al., Uniform flow past one (or two in tandem) finite length circular cylinder(s), *J. Wind Eng. Ind. Aerodyn.* 59 (1996) 69–93.
- [3] T.F. Sun, Z.F. Gu, Interference between wind loading on group of structures, *J. Wind Eng. Ind. Aerodyn.* 54/55 (1995) 213–225.
- [4] T.F. Sun, Z.F. Gu, D.X. He, L.L. Zhang, Fluctuating pressure on two circular cylinders at high Reynolds numbers, *J. Wind Eng. Ind. Aerodyn.* 41–44 (1992) 577–588.
- [5] M. Arie, M. Kiya, M. Moriya, H. Mori, Pressure fluctuations on the surface of two circular cylinders in tandem arrangement, *ASME, J. Fluid Eng.* 105 (1983) 161–167.
- [6] S. Taniguchi, H. Sakamoto, M. Aire, Interference between two circular cylinders of finite height vertically immersed in a turbulent boundary layer, *ASME, J. Fluids Eng.* 104 (1982) 529–536.
- [7] Y. Ohya, A. Okajima, M. Hayashi, Wake interference and vortex shedding, in: *Encyclopedia of Fluid Mechanics*, vol. 8, Ch. 10, 1986, pp. 324–389.
- [8] A. Bokaian, F. Geoola, Wake induced galloping of two interfering circular cylinders, *J. Fluids Mech.* 146 (1984) 383–415.

- [9] M.M. Zdravkovich, D.L. Pridden, Interference between two circular cylinders: series of unexpected discontinuities, *J. Ind. Aerodyn.* 2 (1977) 255–270.
- [10] T.F. Sun, Z.F. Gu, Interference between wind loading on group of structures, *J. Wind Eng. Ind. Aerodyn.* 54/55 (1995) 213–225.
- [11] S. Ishigai, E. Nishikawa, K. Nishimura, K. Cho, Experimental study of structure of gas flow in tube banks with tube axes normal to flow (Part 1, Karman vortex flow around two tubes at various spacings), *JSME* 15(86) (1972) 949–956.
- [12] M.M. Zdravkovich, Review of interference-induced oscillations in flow past 2 parallel circular cylinders in various arrangements, *J. Wind Eng. Ind. Aerodyn.* 28 (1988) 183–200.
- [13] W. Zhang, W.H. Melbourne, Interference between two circular cylinders in tandem in turbulent flow, *J. Wind Eng. Ind. Aerodyn.* 41–44 (1992) 589–600.
- [14] A. Okajima, K. Sugitani, T. Mizota, Flow around a pair of circular cylinders arranged side by side at high Reynolds numbers, *Trans. JSME* 52 (480) (1986) 2844–2850.
- [15] S.J. Price, M.P. Paidoussis, The aerodynamic forces acting in groups of two and three circular cylinders when subject to a cross-flow, *J. Wind Eng. Ind. Aerodyn.* 17 (1984) 329–347.
- [16] Y. Tanida, A. Okajima, Y. Watanabe, Stability of a circular cylinder oscillating in uniform flow or in a wake, *J. Fluid Mech.* 3 (1989) 481–508.
- [17] A.T. Sayers, Flow interference between three equispaced cylinders when subjected to a cross flow, *J. Wind Eng. Ind. Aerodyn.* 26 (1987) 1–19.
- [18] P.W. Bearman, A.J. Wadcock, The interaction between a pair of cylinders normal to a stream, *J. Fluid Mech.* 61 (1973) 499–511.
- [19] M. Kiya, M. Arie, H. Tamura, H. Mori, Vortex shedding from two circular cylinders in staggered arrangement, *ASME, J. Fluids Eng.* 102 (1980) 166–173.